Earth Sciences
2021; 10(5): 207-213
http://www.sciencepublishinggroup.com/j/earth
doi: 10.11648/j.earth.20211005.12
ISSN: 2328-5974 (Print); ISSN: 2328-5982 (Online)

Investigation of the Effect of Strength Anisotropy on Slope Stability of C.D.G.S

Tae-Gew Ham[1, *], Jin-Hwan Lim[2], Man-Bok Ha[3]

[1]Asahitechno CO., LTD, Kitakami-shi, Japan

[2]Depterment of Civil Engineering, Kunsan National University, Gunsan, Republic of Korea

[3]Depterment of Civil Engineering, Gyeongsang National University, Jinju, Republic of Korea

Email address:

hamtg@naver.com (Tae-Gew H.), banibini@hanmail.com (Jin-Hwan L.), doro3000@hanmail.net (Man-Bok H.)

[*]Corresponding author

To cite this article:

Tae-Gew Ham, Jin-Hwan Lim, Man-Bok Ha. Investigation of the Effect of Strength Anisotropy on Slope Stability of C.D.G.S. *Earth Sciences.* Vol. 10, No. 5, 2021, pp. 207-213. doi: 10.11648/j.earth.20211005.12

Received: September 6, 2021; **Accepted**: September 30, 2021; **Published**: October 12, 2021

Abstract: The weathering of the granite rock results in C.D.G.S (completely decomposed granite soil) in most land area. Therefore, the C.D.G.S is commonly encountered in construction field, such as riverbanks and embankments, including roads and railways, and has a stress history of compaction with their construction. In this process, the compacted soil possesses an anisotropic property. Measurement of stress-strain-strength behavior of anisotropic decomposed granite soil is very important for the analysis of deformation and stability of slopes, retaining walls and excavations. Therefore, Anisotropy of mechanical properties for C.D.G.S (compacted decomposed granite soil), a series of unsaturated and saturated-drained triaxial compression tests was performed in order to investigate the deformation and strength anisotropy of C.D.G.S (compacted decomposed granite soils). Three different orientation angles of the axial direction of samples with respect to the horizontal plane were investigated: δ=0, 45 and 90 degrees. As the results showed, the compression strain of specimens subjected to an isotropic compression was influenced strongly by δ. The effect of the angle δ on the strength was more pronounced on unsaturated specimen as compared to saturated specimen. In addition, the time dependence was independent of the settling angle associated with the deformation behavior during the secondary compression process. The effect of settling angle on triaxial compressive strength and deformation was clearly demonstrated at low constraining stresses. Furthermore, to investigate the effect of strength anisotropy according to the height of the fill on the slope stability, slope stability analysis was performed assuming 10m, 20m, 50m, and 100m of the embankment. it became clear that by considering strength anisotropy, the stability of embankment decreased when water level within the embankment was low. In order to obtain more reliable results in the future, verification using various samples will be required.

Keywords: Anisotropy, C.D.G.S (Completely Decomposed Granite Soil), Unsaturated Strength, Sedimentation Plane, Slope Stability Analysis

1. Introduction

The weathering of the granite rock results in C.D.G.S (completely decomposed granite soil) in most land area. Therefore, the C.D.G.S is commonly encountered in construction field, such as riverbanks and embankments, including roads and railways, and has a stress history of compaction with their construction. In this process, the compacted soil possesses an anisotropic property. Much laboratory work has been conducted to find the compressibility or mechanical properties of compacted materials. For compacted specimens employed in conventional triaxial tests, the direction of the compaction loading corresponded with the direction of the major principal stress. However, the stress conditions in a soil structure caused by additional loading, such as an earthquake, should vary in terms of the direction of the major principal stress. Therefore, in order to study stability and deformability of a structure using compacted materials, it is necessary to understand the anisotropic properties for the

unsaturated compacted material. Although it has been widely recognized, studies of the anisotropic property of compacted materials have been limited to clayey soils [7, 12]. Conversely, saturated clay and soil have been studied by many researchers (e.g., [1-5, 8-10, 14, 17]), but previous researches concerning anisotropic property of C.D.G.S materials are limited. Therefore, it is necessary to collect substantial data in order to understand the mechanical properties of C.D.G.S. A series of unsaturated-drained triaxial compression tests were performed on unsaturated compacted materials. The tests were planned to find not only the degree of anisotropy for the sedimentation angle of the compacted material, but also the influences of the confining stress, degree of saturation and specimen preparation method on the anisotropic properties. The test results show not only the degree of anisotropy considering the sedimentation angle of the compacted material, but also the influence on the unsaturated C.D.G.S materials.

2. Indoor Test

2.1. Material Properties

The physical properties of the sample are shown in Table 1, and the grain size distribution curve of the materials in Figure 1. Matsuo et al. [10] confirmed that the higher the degree of weathering, the higher the moisture content, and that specific surface area, ignition loss, and absorption rate are effective indicators for evaluating the weathering degree of granite weathered soil.

Table 1. *Physical properties of soils used.*

Sample	Max. Grain size (mm)	G_s	Ignition loss (%)	U_c	w_{opt}	ρ_{dmax} (g/cm^3)
Shimonoseki	< 2	2.68	1.83	7.14	13.24	1.78

Uc is the coefficient of uniformity, and the degree of weathering was determined from ignition loss. Quartz, feldspar, and colored mineral contents of this sample were about 23, 62 and 15%, respectively. Ignition loss of Toyoura sand, mostly composed of quartz, with a small degree of weathering, was 0.4. The ignition loss Myoung-Gyu Lee, et al [9] of the sample was 1.83.

2.2. Method

Decomposed granite soil with optimum moisture content (w=13%) was compacted in a container (200 mm×100 mm×200 mm) by hitting with a 19.6N rammer. The density of the compacted materials was controlled by the relative compaction, R, to be 90%. The relative compaction was defined as the percentage of the density to the maximum dry density obtained from each compaction test. The soils are compacted by 1.8 cm at each layer to make 20 cm height. The rectangular sample was frozen at under -20°C followed by cylindrical triaxial compression of the specimens into a 50 mm diameter and 100 mm height using a core bit machine, as shown in Figure 2. The liquefied nitrogen was sprinkled to the sample with 80 kPa to avoid disturbance. The sample had three different angles of the axial (major principal) direction to the sedimentation plane (compaction plane): 0, 45 and 90 degrees. Specimens were set up under a 20 kPa confining pressure, with melting for about 6-hours. After this, confining pressures up to, 30, 60, 120 or 240 kPa were applied for 1 or 10 hours, in order to find the time dependency of the mechanical behavior of the unsaturated compacted materials.

The first set of specimens was similar to the frozen specimens used in the triaxial tests. For comparison purposes, the second set of specimens consisted of compacted soils having different initial degrees of saturation, Sr, ranging from 40-90%.

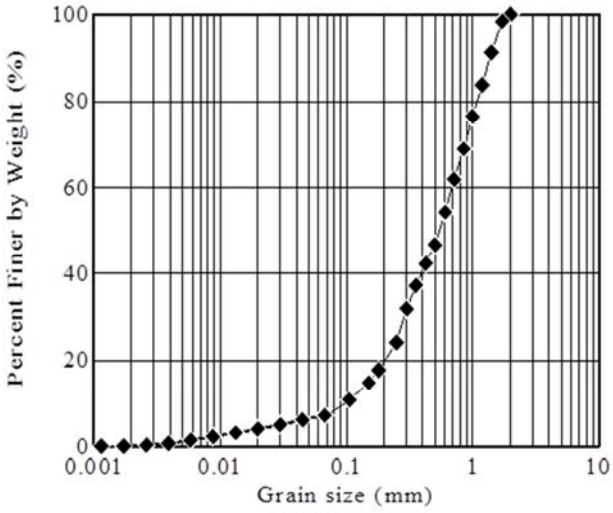

Figure 1. *Grain-size distribution curves of soils used.*

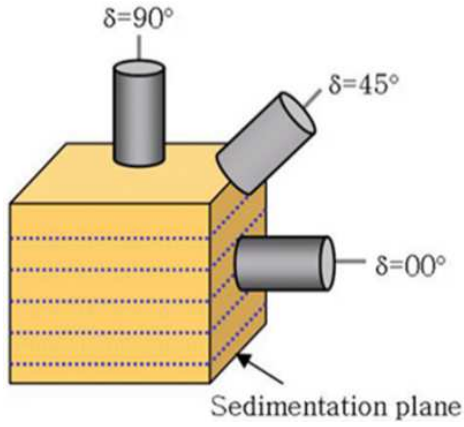

Figure 2. *Schematic diagram of showing angles ofaxial direction δ with respect to the bedding plane.*

3. Indoor Test Result

3.1. The Effect of the Angle of Sedimentation on the Compression Settlement

Figure 3 Show the relationship between the elapsed compression time and the axial strain for a sample subjected to a 60kPa confining stress. There were two compression processes; one was the primary compression process, from the beginning to the end of the confining pressure loading, and the other the secondary compression process, after the end of the confining pressure loading. The amounts of axial strain during the primary and secondary compressions were referred to as S_1 and S_2, respectively, as shown in Figure 3.

The isotropic compression behavior, S_1, increased suddenly due to the immediate settlement during the primary compression process, after then S_2 showed only a slight non-linear relationship with the function of the logarithm of time during the secondary compression process.

Figure 4 Show the relationship between the axial strain and time under the conditions of 60kPa of confining pressure and 10 hours compressive stress. The arrow in the Figure 4 represents the moment the load ended. As δ of the specimen decreased from 90° to 0°, the axial strain S_1 increased.

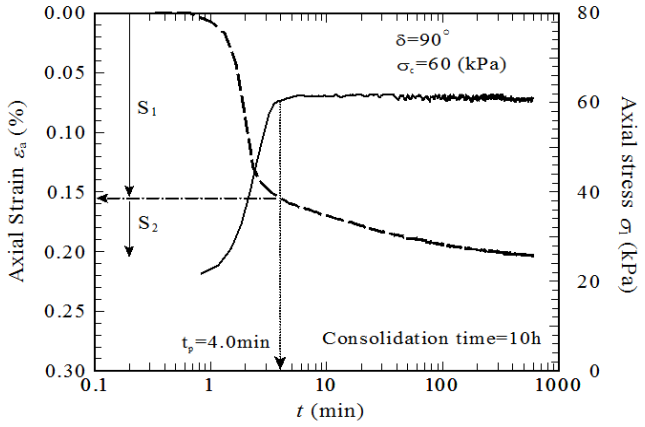

Figure 3. *Relationship between axial strain, axial load and time of compression (δ=90°).*

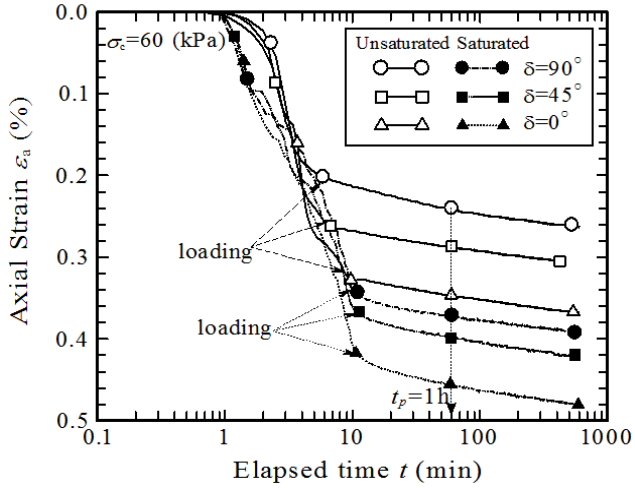

Figure 4. *Relationship between axial strain and time of compression.*

Figure 5 shows the effect of the confining pressure on the relationship between the axial strain and the duration of compressive stress for samples subjected to30, 60, 120, 240kPa confining pressures for specimens with δ =90°. As the confining stress increased, the amount of axial strain S_1 also increased. The arrows in the Figure 5 represent the moment the load ended. Then, the amount of axial strain, S_2, was approximately the same for all confining stresses. The behavior of deformation during the secondary compression process was verified as not having any dependency on the confining stress. S_2 was considered to be related to the particle rearrangement and decreased suction factors that were the result of the compression.

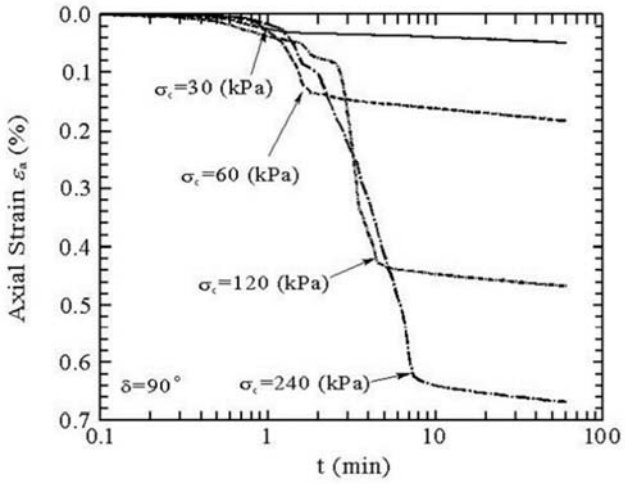

Figure 5. *Relationship between Axial strain and compression time (min).*

3.2. The Effect of the Angle of Sedimentation on the Strength

In order to investigate the shear property of the compacted specimen with 90, 45 and 0 degree angles of sedimentation, drained triaxial compression tests were performed. The deviator stress-axial strain and axial-volumetric strains diagrams for the specimen compressed at 120kPa are shown in Figure 6. The deviator stress showed a clear maximum stress points, which then slowly decreased as shown in Figure 8. As the value of δ increased from 0° to 90°, the maximum value of the deviator stress q_{max} also increased, but the axial strain at q_{max} decreased. In addition, the dilatancy rate at the point of failure increased with increasing δ . Figure 7 shows the change in the deviator stress obtained for strains up to 0.05% for the specimens.

Immediately after conducting the shear test, all specimens showed almost the same behavioral characteristics until around 0.005% of the axial strain rate, and the dependence on saturation and value of δ was not confirmed. This is the same as the results of the study conducted by Tatsuoka et al. [15], Tatsuoka et al. [16] and Kohata et al. [6], and means that no movement between particles occurs and elastic particle deformation is dominant in the range of micro-strain (0.005% or less) of the C.D.G.S.

Figure 8 shows the relationship between shear strength (τ), total stress (σ), and effective stress (σ') calculated by the

Mohr-Coulomb fracture criterion for the results of unsaturated and saturated specimens. Figure 9 is Figure 8 shows the relationship between the adhesive force (c), the internal friction angle (Φ'), and the angle (δ) between the σ1 direction and the deposition surface. From Figure 9 it can be seen that the internal friction angle (Φ') also increases as δ increases for both saturated and unsaturated specimens regardless of the degree of saturation, and the amount of increase is constant regardless of the degree of saturation.

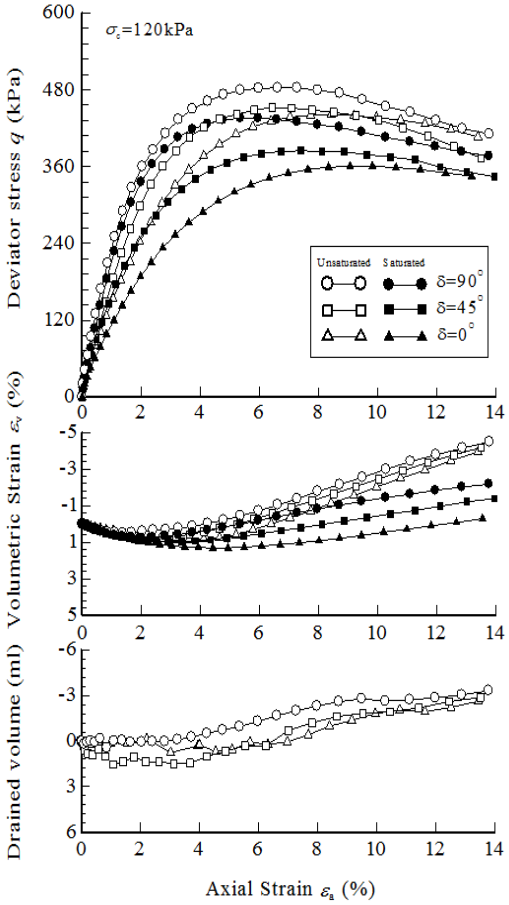

Figure 6. *Relationship between axial strain and deviator strain, volumetric strain and drain volumetric strain.*

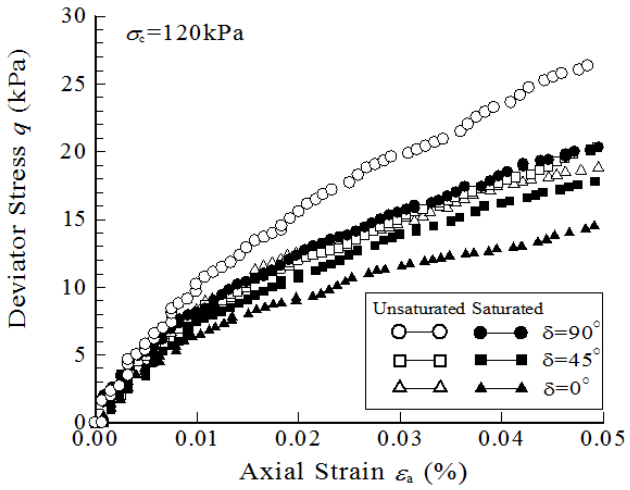

Figure 7. *Stress- strain relations (up to ε_a=0.05%).*

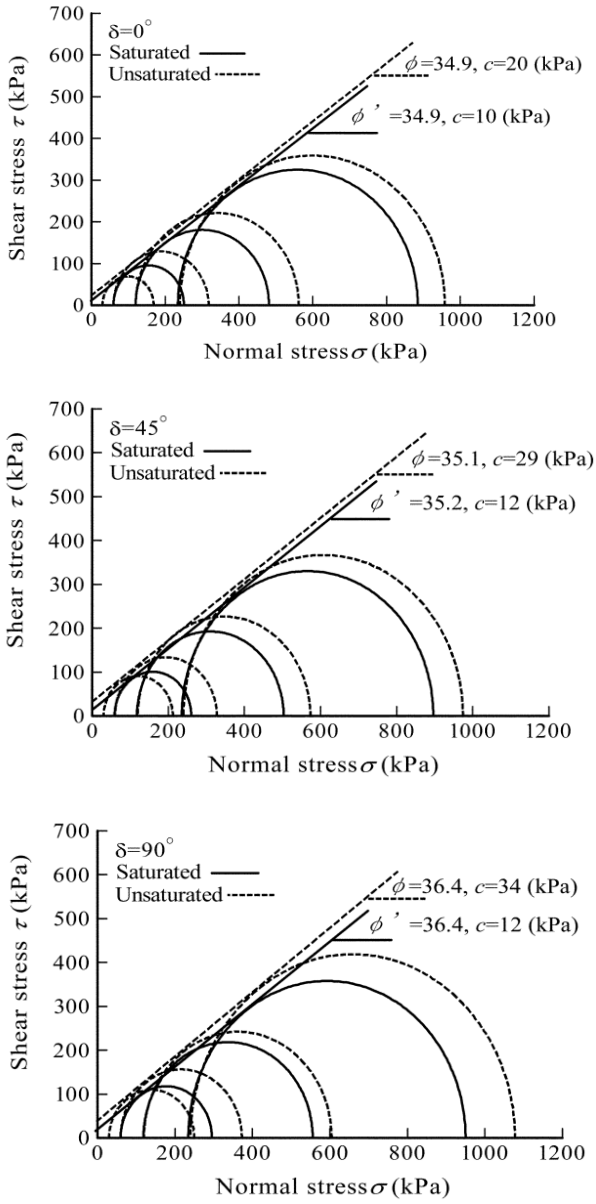

Figure 8. *Strength constant obtained by Mohr-Coulomb fracture criterion.*

In addition, the saturated specimen shows a constant value regardless of the change in δ, whereas the unsaturated specimen shows a tendency to increase the adhesive strength as δ increases from 0° to 90°. This result means that the suction force acting on the unsaturated specimen serves to increase the adhesive force, and the apparent adhesive force increased due to the suction force depends on δ.

Figure 10 shows the relationship between the secant shear resistance angles at peak shear stress (φ_{peak}) and the mean principal stress, p. As the mean principal stress increased, φ_{peak} decreased steeply.

The slope became steeper as δ became large. The effect of the angle of sedimentation on the strength of deformation was clear with low mean principal stress. In the case of Ube, the tendency for a steep slope was shown to be very gentle with increases in the mean principal stress, p, compared with the data of Shimonoseki.

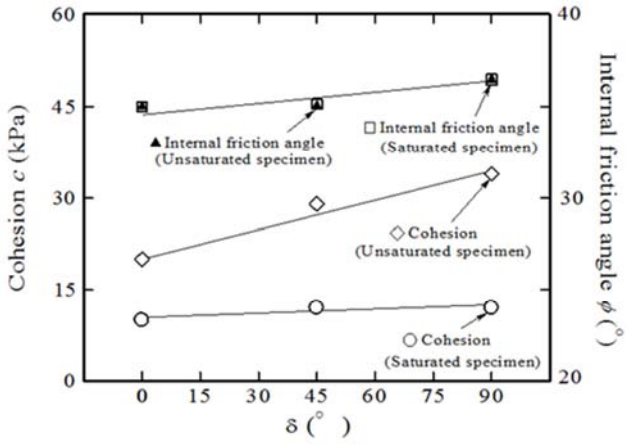

Figure 9. *Relationship among cohesion, internal friction angle and* δ .

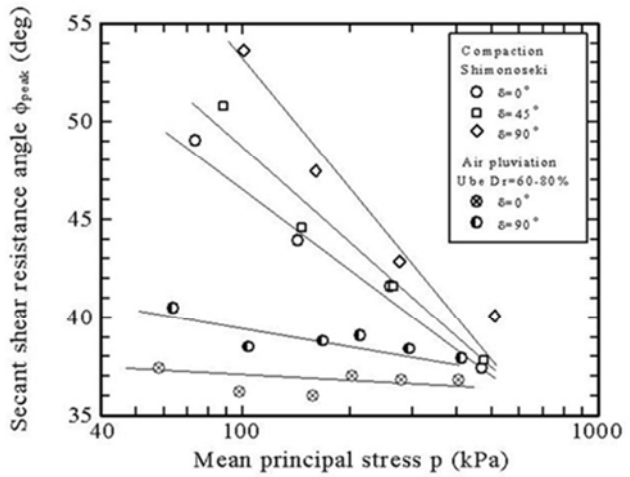

Figure 10. *Relationship between secant shears resistance angles at peak shear stress and mean principal stress.*

It was thought that the initial fabric arrangement would remain nearly constant in a low confining stress. As the confining stress increased, the particles were rearranged by particle breakage, such that the effect of the angle of sedimentation disappeared under high confining stress.

3.3. The Effect of the Angle of Sedimentation on the Dilatancy

In order to show the effect of the angle of sedimentation on the dilatancy, the ratio of the volumetric strain increment to the increment of the axial strain at peak stress conditions, $(-d\varepsilon_v / d\gamma)_{peak}$, was examined. Figure 11 shows the ratio of $(-d\varepsilon_v / d\gamma)_{peak}$ for an angle of sedimentation to $(-d\varepsilon_v / d\gamma)_{peak}$ for a δ of 90°. The ratio $(-d\varepsilon_v / \varepsilon\gamma)_{peak}$ / $(-d\varepsilon_v / \varepsilon\gamma)_{peak}$ at =90° was plotted against δ . As the confining stress increased, the ratio, $(-d\varepsilon_v / d\gamma)_{peak}$ /{ $(-d\varepsilon_v / d\gamma)_{peak}$ at δ =90°} decreased. The $(-d\varepsilon_v / d\gamma)_{peak}$ /{ $(-d\varepsilon_v / d\gamma)_{peak}$ at δ =90°)} with a confining stress of 30kPa was 0.58. As the confining stress increased, the value of $(-d\varepsilon_v / d\gamma)_{peak}$ /{ $(-d\varepsilon_v / d\gamma)_{peak}$ at =90°)} was approximately 1.0.

The C.D.G.S had lower values of { $(-d\varepsilon_v / d\gamma)_{peak}$ at δ =0°} /{ $(-d\varepsilon_v / \varepsilon\gamma)_{peak}$ at δ =90°} than the data for the air pluviated decomposed granite and Toyoura sand. Figure 12. shows the relationship between the increment of strength due to dilatancy, $\varphi_{peak} - \varphi_{cv}$, and the dilatancy rate, $(d\varepsilon_v / d\gamma)_{peak}$ at failure. As $(d\varepsilon_v / d\gamma)_{peak}$ increased, $\varphi_{peak} - \varphi_{cv}$ also increased. The same tendency was obtained for all specimens used in this paper.

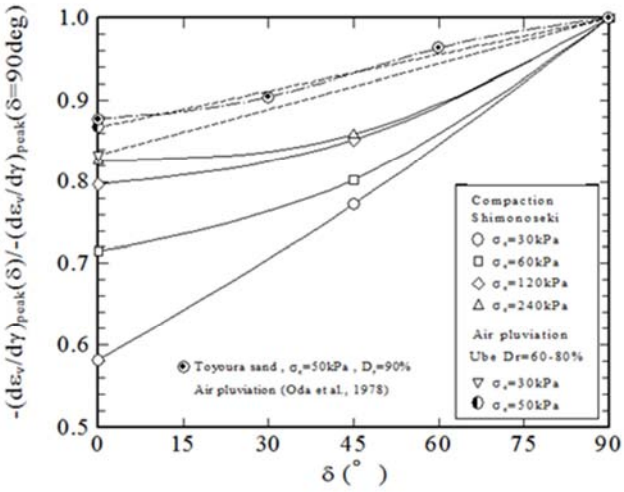

Figure 11. *{ $(-d\varepsilon_v / d\gamma)_{peak}(\delta)$ }/{ $(-d\varepsilon_v / d\gamma)_{peak}$ for a δ of 90°}.*

3.4. Effect of Strength Anisotropy on Embankment Height on Slope Stability

In order to investigate the effect of strength anisotropy on the stability of the slope due to the embankment height, assumed an embankment with different heights of 10 m, 20m, 50m, and 100m, and performed a slope stability analysis.

Figure 13 Shows the cross-sectional view of the embankment used for slope stability analysis.

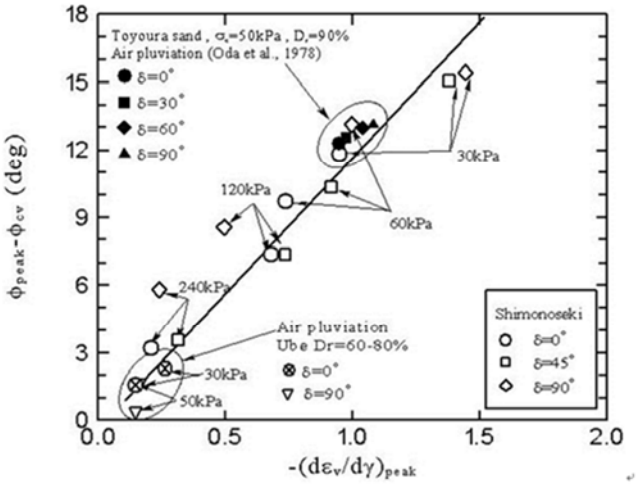

Figure 12. *Relationship between ($\varphi_{peak} - \varphi_{cv}$) and $-(d\varepsilon_v / d\gamma)$.*

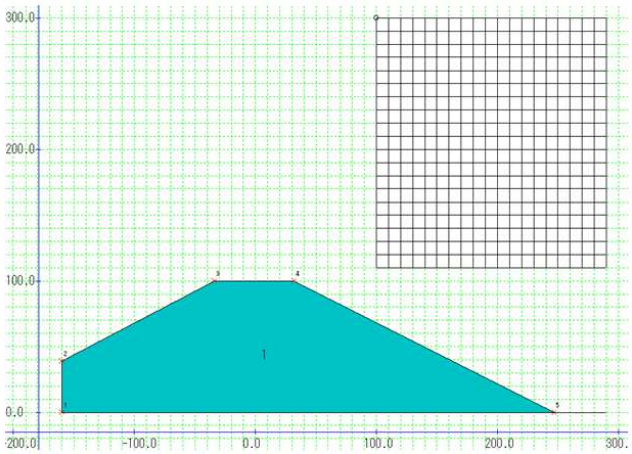

(a) Slope stability analysis by Fellenius method

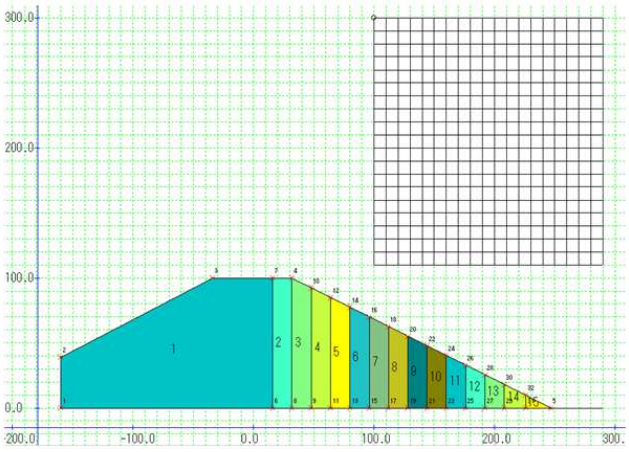

(b) Slope stability analysis considering anisotropy

Figure 13. *Cross section used for slope stability analysis.*

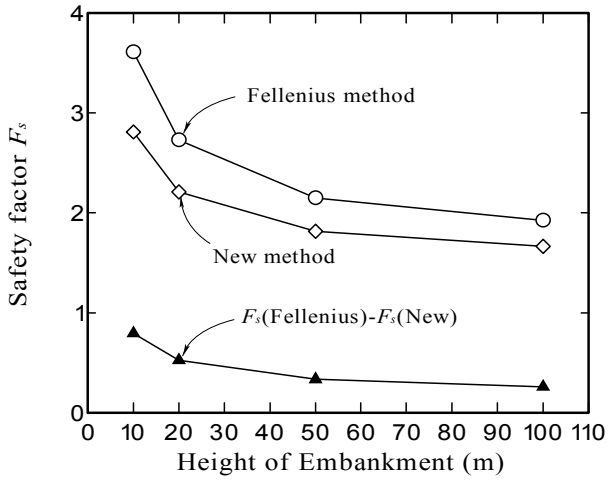

Figure 14. *Results of slope stability analysis considering the Fellenius method and anisotropy (effect of embankment height).*

In order to investigate the effect of strength anisotropy on the stability of the slope, the groundwater level in the embankment was changed to 10m, 30m, 50m, 91.9m, and conventional slope stability analysis considering anisotropy were performed carried out. The simplest and long-used simple division method (Fellenius method) is used as the stability analysis method used this time.

Figure 14 shows the relationship between the embankment height and the safety factor, which is the result of the slope stability analysis calculation performed. From the Figure 14, it can be seen that the safety factor obtained by considering the conventional Fellenius method and anisotropy decreases as the embankment height increases. In addition, the safety factor obtained in consideration of anisotropy is smaller than the safety factor obtained by the conventional Ferrenius method, and the difference is Fs(Ferenius method) -Fs(new method). The value decreases as the height of the embankment increases. This is thought to be because the higher the embankment height, the less the effect of suction on the stability of the embankment.

From the above results, the effect of strength anisotropy on the stability of the embankment slope is greater in soil structures with low embankment height, and the assumption of anisotropy of strength constants reveals more dangerous results. Furthermore, it became clear that by considering strength anisotropy, the stability of embankment decreased when water level within the embankment was low. In order to obtain more reliable results in the future, verification using various samples will be required.

4. Conclusion

This paper introduces a series of unsaturated-drained triaxial compression tests which were performed on C.D.G.S (completely decomposed granite soils). Typical testresults from a series of triaxial tests for unsaturated samples were planned to find the effect of not only angle of sedimentation, but the influence of confining stress, degree of saturation and specimen preparation method on the anisotropic properties. Following conclusions may be drawn.

The Secant Young's modulus showed the same behavior for all specimens, even with different δ

The effects of the angle of sedimentation on the triaxial compression strength and deformation were clearly generated at the low confining stress than at the high confinement stress.

The difference between the peak strength φ_{peak} and the residual strength φ_{cv} was dominated by the dilatancy for compacted specimens.

The compacted specimen can be considered to have anisotropic mechanical properties, the same as the initial fabric anisotropy of sand.

The effect of strength anisotropy on the stability of the fill slope is greater for geologic structures with low fill heights, and assuming an anisotropy of the strength constant gives more dangerous results. In order to confirm these results in the future, verification using various samples will be required.

References

[1] A. J. Hendron. (1963). The behavior of sand in one-dimensional compression. Ph.D. thesis, Univ. of Illinois at Urbana Champaign, Urbana, Ill., 50–89.

[2] J. M. De Souza (1958). Compressibility of sand under high pressure. MS thesis, Massachusetts Institute of Technology, Cambridge, Mass., 63–64.

[3] J. A. Yamamuro, and P. V. Lade. (1996) Drained behavior in axisymmetric tests at high pressures. J. Geotech. Engrg., 122 (2), 109–119.

[4] Jiyeon Choi, Sanghwa Oh, Jeong-Hun Park, (2014) Inseong Hwang (2014) Evaluation of CODsed Analytical Methods for Domestic Freshwater Sediments: Comparison of Reliability and Correlationship between CODMn and CODCr Methods Journal of Environmental Science International Vol. 23 No. 2 pp. 181-192**.**

[5] K. Terzaghi, and R. B. Peck. (1948) Soil Mechanics in engineering practice, Wiley, New York, 65–67.

[6] Kohata, et al. (1995): Inherent and induced anisotropy of sedimentary soft rock, *Proc. of 10ARC,* pp. 33–36.

[7] Livneh, M. and Komornik, A. (1967) Anisotropic strength of compacted clay, Proc., 3rd ASIAN Reg. Conf. On SMFE, Vol. 1, pp. 298-304.

[8] M. M. Hagerty, D. R. Hite, C. R. Ullrich, and D. J. Hagerty.(1993) One dimensional high pressure compression of granular media. J. Geotech. Engrg., 119 (1), 1–18.

[9] Myoung-Gyu Lee, Ji Hoon Kim, (2006) Numerical Implementation of Modified Couomb-Mohr Yiedl Criterion for Anisotropic Materials. Fibers and Polymers Vol 7, No. 3, 276-285.

[10] Matsuo, S., Nishida, K., and Sasaki, S. "Physical properties of weathered granite soil particles and their effect on permeability." Soil Found., 19 (1), 13–22. (1979).

[11] Nakata, Y., Hyodo, M. and Murata, H.(1998) Single particle crushing and mechanical behavior of decomposed granite soil, Proceedings of the international symposium on problematic soils, IS-TOHOKU'98. SENDAI, JAPAN: pp. 483-497.

[12] Onitsuka, K. and Hayashi, S., (1979) Studies on compression and strength Anisotropy of compacted soils, in Japanese. JSCE. Vol. 19, No. 3, Sept, pp. 113-123.

[13] Oda, M., Koishikawa, I., and Higuchi, T., (1978) Experimental study of anisotropic shear strength of sand by plane strain test, Soils and Foundation, Vol. 18, No. 1, pp. 25-38.

[14] P. V. Lade, and J. A. Yamamuro. (1996) Undrained sand behavior in axisymmetric tests at high pressures. J. Geotech. Engrg., 122 (2), 120–129.

[15] Tatsuoka, F., Nakamura, S., Huang, C. and Tani, K.,(1990) Strength anisotropy and shear band direction, Soils and Foundation, Vol. 30, No. 1, pp. 35-54.

[16] Tatsuoka, F. amd Shibuya, S., (1992) Deformation characteristics of soils and rocks from field and laboratory tests, Keynote Lecture, Proc. of 9th Asian Regional Conf. on SMFE, Vol. 2, pp. 101-170.

[17] Y. Nakata, M. Hyodo, A. F. L. Hyde, Y. Kato, and H. Murata. (2001) Microscopic particle crushing of sand subjected to high pressure one-dimensional compression. Soil Found. 41 (1), 69–82.